Iranian Journal of Science & Technology, Transaction B, Engineering, Vol. 33, No. B1, pp 15-30
Printed in The Islamic Republic of Iran, 2009

SWELLING AND DIFFUSION CHARACTERISTICS OF THE EXPERIMENTAL GCLs*

K. BADV** AND R. FARSIMADAN

Dept. of Civil Engineering, Urmia University, Urmia, I. R. of Iran
Email: k.badv@urmia.ac.ir

Abstract– Swelling and diffusion characteristics of GCL samples made in the laboratory were studied and the results compared with the results of an industrial GCL. A Swell-Diffusion apparatus was designed, fabricated, and used to perform the swelling and swelling-diffusion tests. Two types of available local geotextiles (Types I and II) with an available low quality Bentonite (LQB) were used to fabricate two types of GCL's in the laboratory (Types A and B E-GCLs). The effect of stitching, applied stress, and wetting procedure, was investigated in swelling tests. For type A E-GCL, with no stitch and no applied stress, a maximum of 6 mm swell was observed. Under 12.5 kPa stress, the swell decreased to a maximum of 2 mm. When this GCL was stitched, a maximum of 1.8 mm and 1.4 mm swell with zero and 12.5 kPa stresses were shown, respectively. The swelling results showed that the wetting procedure (from top, from bottom, and both ways) has a negligible effect in maximum swell. The type B E-GCL (having better geotextile quality compared to type A) showed a maximum 2.3 mm swell with no stitch, and 1.6 mm swell when stitched. The industrial needle punched reinforced GCLs with high quality granular sodium bentonite, under 12.5 kPa stress and wetted from top and bottom, showed a maximum of 3 mm swell. The swell data obtained from these experiments are in reasonable agreement with the data reported in the literature for similar GCLs under comparable conditions.

Diffusion experiments were performed for types A and B E-GCL's, as well as for the industrial GCLs. The chloride diffusion coefficients for types A and B E-GCL's ranged from 2.7×10^{-10} m^2/s to 3.5×10^{-10} m^2/s compared to 2.9×10^{-10} m^2/s to 3.5×10^{-10} m^2/s for the industrial GCLs, which is in good agreement.

Keywords– Swell, diffusion, laboratory-made GCL's, stitching, wetting, stress

1. INTRODUCTION

Geosynthetic clay liners (GCLs) have gained growing recognition as an alternative to a conventional compacted clay liner in the base seals of landfills [1-3]. The design of waste disposal facilities typically involves some form of barrier that separates the waste from the general groundwater system. This barrier is intended to minimize the migration of contaminants from the facility [4, 5]. Engineered municipal solid waste landfills rely on a base liner system to mitigate contaminant migration from the landfill into the underlying hydrogeological environment [6-8]. Traditionally, base liner systems such as natural clayey deposits and compacted clay liners (CCLs) have been utilized to minimize contaminant transport through the barrier system [8, 9]. In some areas economic use of low hydraulic conductivity clay is not possible and hence geosynthetic clay liners are used in place of, or in combination with, a clayey barrier to provide the low hydraulic conductivity of the liner system required by various regulatory authorities [10-12].

The characteristics and performance of the GCLs have been investigated from several different viewpoints in the technical literature. In summary, the hydraulic conductivity [13, 14], swelling [15, 16], diffusion [13, 17, 18], freeze-thaw [19, 20], method of production (e.g., this study), stress level [21], and component material type (type of Bentonite and encapsulating geotextiles) [22, 23] have been the focus of many researchers.

*Received by the editors August 13, 2007; Accepted September 14, 2008.
**Corresponding author

The Environmental Geotechnique Research Laboratory of Urmia University, Iran, was awarded a research grant to investigate the potential for the production of some GCLs in laboratory scale (called Experimental GCLs, E-GCLs), using the available local material. Then, some index, swelling, and diffusion tests on the produced specimens were demanded. The experimental program included three components. First, using local geotextiles and bentonite products, some GCL specimens were fabricated in the laboratory in such a way that the produced specimens have a quality comparable to similar industrial products. Second, some index tests were performed on the bentonite and fabricated GCLs. Third, a swell-diffusion apparatus was designed and fabricated to perform swell and diffusion tests on the GCL specimens. The results have been discussed in the following sections.

2. CHARACTERISTICS OF THE EXPERIMENTAL GCLs

a) Bentonite

A sodium bentonite produced by the Iran Barit Company, Iran, was used to fabricate E-GCLs. Some granular sodium bentonite was exhumed from Bentofix-NW geotextile (BENTOFIX®, product No. FIX-501NW, the term "industrial geotextile" will be used, as described in section 3) and index tests were performed on both bentonite samples for comparison. The index tests included an XRD test, free swell test (ASTM D5890), and Methylene Blue adsorption test [24]. The results are shown in Table 1. The XRD test showed that the largest mineral fraction in both bentonite samples is Montmorillonite with smaller fractions of Calcite and Quartz. The CEC of the sodium bentonite is 77 meq/100g compared to 84 meq/100g for exhumed bentonite. The S_s of sodium bentonite is 600 m^2/g compared to 636 m^2/g for exhumed bentonite. These data show that the sodium bentonite used in this study is verified as low quality bentonite [23].

Table 1. Characteristics of sodium bentonite and exhumed bentonite

Properties	Sodium Bentonite	Exhumed Bentonite
Montmorillonite content (%)	76	73
Liquid limit (%)	307	550
Plastic limit (%)	49	60
Cation exchange capacity (CEC, meq/100g)	77	84
Specific surface (S_s, m^2/g)	600	636
Swell index (mL/2g)	33	30

b) Geotextiles

Two types of geotextiles were used to fabricate the E-GCLs which will be referred to as type I and type II. The nominal thickness of type 1 and type 2 geotextiles were 3.5 mm and 2.5 mm, respectively. The unit weight, the weight per unit area, and thickness under average applied stress of 12.5 kPa were measured for the geotextiles as listed in Table 2. The 12.5 kPa stress represents conditions where the GCL hydrates under about 0.6 m of cover material.

Table 2. Characteristics of the geotextiles used in E-GCLs fabrication

Type of geotextile	Unit weight (g/cm^3)	Weight per unit area (Minimum Average Roll Value - g/m^2)	Thickness under average applied stress of 12.5 kPa (mm)
Type I (*Pars Mocket Co.)	1.1	560	2
Type II (*Lay Saz Co.)	1.2	200	1.6

*Local companies which produce types I and II geotextiles used in this study

c) E-GCLs

Two types of E-GCLs (types A and B) were fabricated in the laboratory using two types of geotextiles listed in Table 2, and the sodium bentonite described above. The fabricated E-GCLs types A and B had the weight per unit areas of 5000 g/m^2 and 6000 g/m^2, respectively. To determine the required weight per unit area of the sodium bentonite to be used for the production of E-GCLs, the apparent unit weight of the sodium bentonite was measured by pouring the bentonite into a container with no compaction. Then, by dividing the weight of the bentonite to its volume, the apparent unit weight was determined. The target weight per unit area of the E-GCLs after fabrication was considered to be 5000 g/m^2. The weight of the geotextiles was subtracted from the weight of the E-GCLs to determine the weight per unit area of the bentonite. The thickness of the encapsulated bentonite layer was then calculated using the following simple formulas:

$$\gamma = W/V, \qquad V = At, \qquad V = W/\gamma, \qquad t = w/\gamma A$$

Where (γ) is the unit weight of the E-GCL (g/cm^3), (W) is the weight of the bentonite (g), (V) is the volume of the bentonite (volume of the container, cm^3), (A) is the area of the E-GCL (cm^2), and (t) is the thickness of the E-GCL (cm).

During the fabrication process of E-GCLs, a clean surface with a 50 cm by 50 cm area was considered and the carrier geotextile was cut and laid on the surface. Then, layers of foam with the calculated thickness (t) of bentonite were cut and placed around the geotextile to provide an encapsulated area for the bentonite application with the thickness of (t). Then, bentonite was carefully and uniformly poured inside the area surrounded by foam. The final area of the bentonite was flattened by applying a metal ruler on the foam. Then, the cover geotextile was placed on the bentonite and the carrier and cover geotextiles were stitched together in rows about 5 mm apart, in two directions, using a thin polyester yarn. During the stitching process care was taken to avoid any displacement of the encapsulated bentonite. In type (A) E-GCL, the carrier and cover geotextiles were type I geotextiles, and in type (B) E-GCL, the carrier and cover geotextiles were type II geotextiles. Figure 1 shows a picture view of the fabricated E-GCLs. In this figure, two samples of type (A) E-GCL are shown on the top and bottom with black color, and one sample of type (B) E-GCL is shown in the middle with white color.

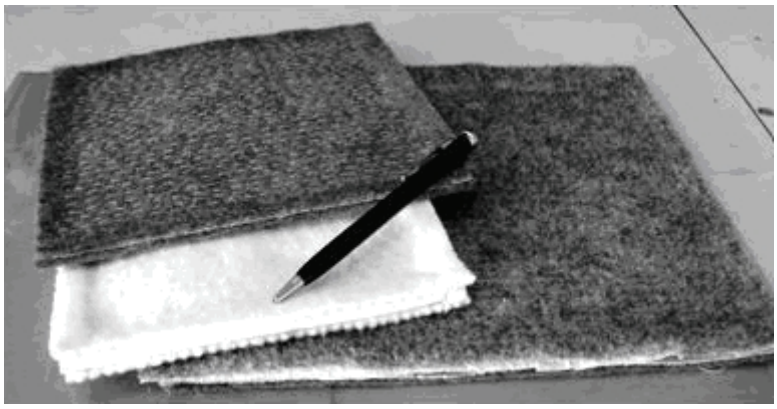

Fig. 1. A picture view of the types (A) and (B) E-GCLs fabricated in the laboratory

3. CHARACTERISTICS OF THE INDUSTRIAL GCLs

Two types of industrial GCLs were used as reference GCLs in this study. The GCL types were Bentofix-NW and Bentofix-NWL supplied by BENTOFIX® with the product Nos. FIX-501NW and FIX-501NWL, respectively. Both GCLs were nonwoven thermally treated needle punched reinforced GCL. Bentofix-NW

and Bentofix-NWL comprised of a uniform 4.34 kg/m^2 and 3.66 kg/m^2 respectively (measured), granular sodium bentonite layer encapsulated between a scrim reinforced nonwoven and a virgin stable fibre nonwoven geotextile with the minimum average roll values of 200 g/m^2. Their minimum bentonite swell indexes were 24 mL/2g (specified) and 30 mL/2g (measured in this study).

4. SWELL-DIFFUSION APPARATUS

A swelling-diffusion Apparatus was designed and fabricated to perform swelling and diffusion tests on GCL samples. The apparatus was designed so that either the individual, the swelling test or the swelling and diffusion test could be performed in this apparatus. Figure 2a shows the sketch of the design, Fig. 2b shows a picture view of the assembled apparatus, and Fig. 3 shows the individual parts of the disassembled apparatus.

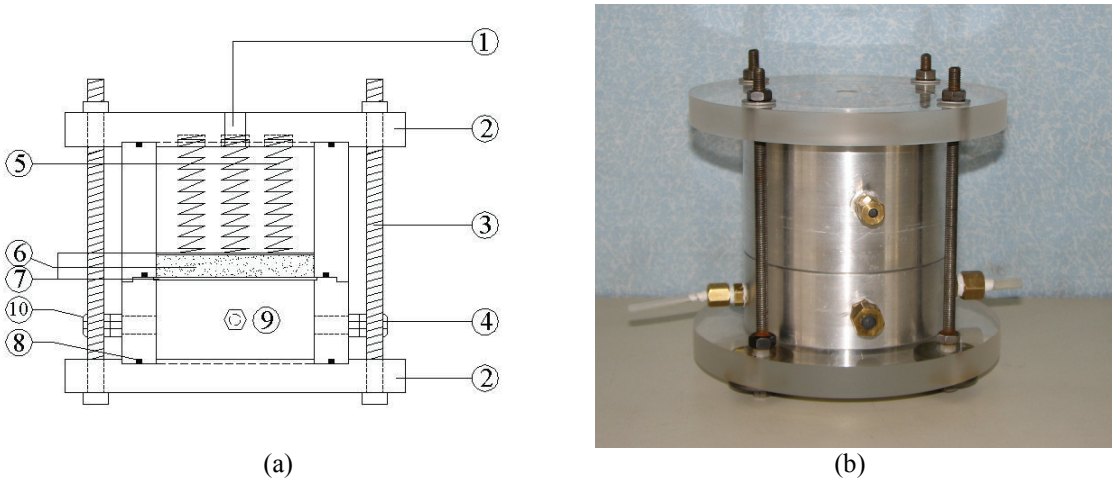

(a) (b)

(1) an opening to install a dial gauge, (2) top and bottom Plexiglas plates, (3) threaded rod, (4) water inlet, (5) spring, (6) GCL sample, (7) perforated plate, (8) o-rings, (9) sampling port, (10) water outlet

Fig. 2. (a) Schematic of swell-diffusion cell, (b) a picture view of the cell

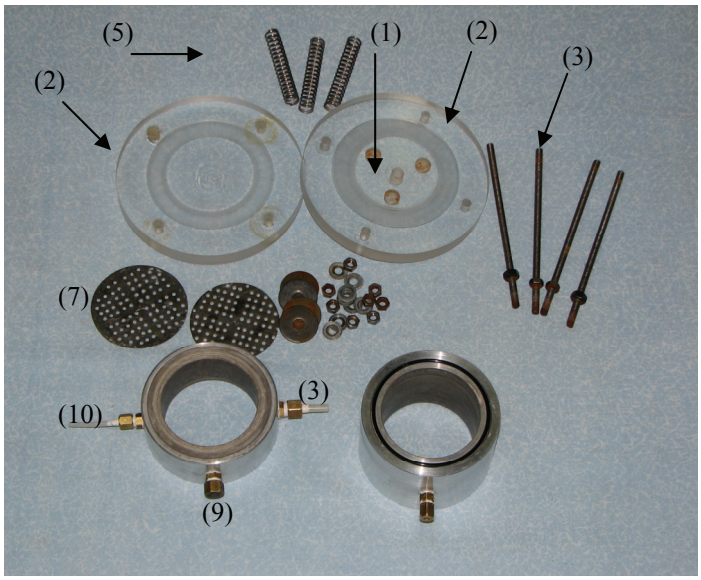

Fig. 3. A disassembled swell-diffusion cell (Numbers are as described in Fig. 2a)

5. SWELL TESTS

In this part of the study the swelling test procedure has been described and the effect of stitching, applied stress and the method of wetting on the E-GCLs have been investigated. Figure 4 shows the tree-diagram for the conducted tests. For type (A) E-GCL, the test numbers will be referred to as A1 to A12. For type (B) E-GCL, the tests referred to as "no stress", "wetting from top", and "wetting from bottom" were not conducted. The conducted test numbers will be referred to as B1 to B4. The industrial GCLs were tested under stress and were wetted from top and bottom. The test numbers for Bentofix-NW will be referred to as tests NW1 and NW2 and for Bentofix-NWL will be referred to as tests NWL1 and NWL2.

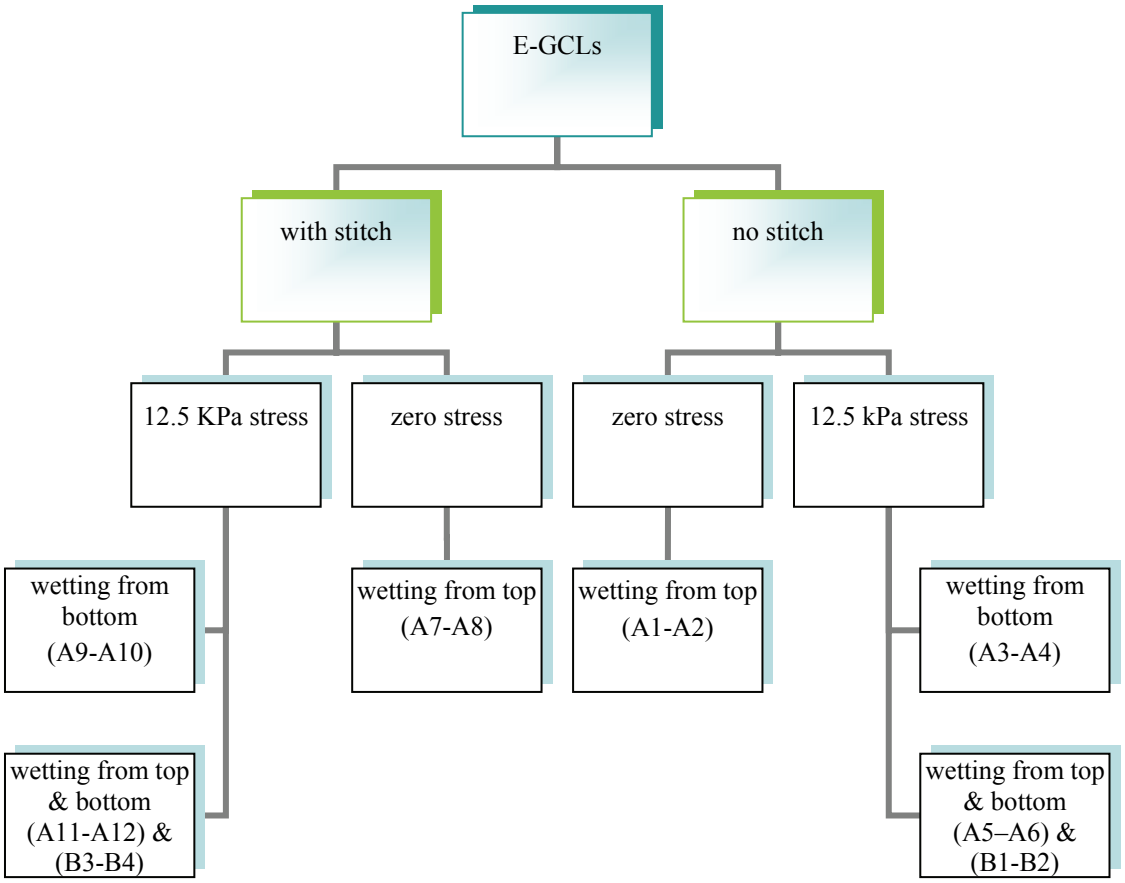

Fig. 4. A tree-diagram showing the conducted swell tests for E-GCLs

a) Test setup

To setup a swell test, the following procedure was adopted. (1) The bottom Plexiglas plate was laid on the table and four threaded rods were attached to the plate. (2) The lower aluminum ring was placed on the table and the lower perforated plate was placed inside the ring. This plate supports the E-GCL. (3) If the stitched E-GCL sample is tested, after fabricating the sample, it was cut into a 7 cm diameter using a cutting ring and a jack system, and the sample was then placed on the perforated plate and the upper perforated plate was placed on the E-GCL. If the un-stitched E-GCL sample is tested, first a 7 cm diameter carrier geotextile was placed on top of the lower perforated plate. The required amount of sodium bentonite was evenly poured on top of the geotextile, then the covered geotextile was placed on the surface of the bentonite, and finally, the upper perforated plate was placed on the covered geotextile. (4) The upper aluminum ring was placed on top of the lower aluminum ring. (5) The pressure springs were placed in their locations (holes) under the upper Plexiglas plate and the plate was placed on top of the

upper aluminum plate. (6) The cell was tightened using the nuts and threaded rods. In this process care was taken to insure that the springs are located vertically inside the cell. (7) A plastic tank containing distilled water was attached to the lower aluminum ring through the water inlet and water was allowed to flow inside the ring and exit through the water outlet to de-air the lower ring. After the de-airing process, the outlet valve was closed. (8) The cell was levelled on the table, a dial gauge was assembled on a stand and its arm was positioned on the top of the upper perforated plate (on top of the E-GCL) inside the upper aluminum ring through the opening of the top Plexiglas plate. (9) The recording of the swelling of E-GCL commenced immediately after the dial gauge assembly and was continued until no further swell was observed. Figure 5 shows the swell test setup for the "wetting from bottom" test.

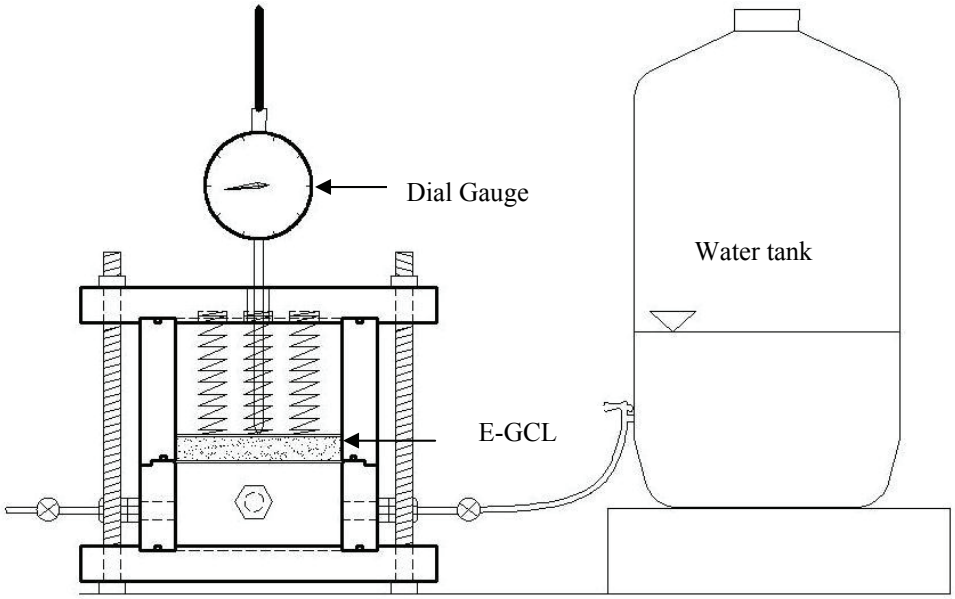

Fig. 5. Schematic of the swell test setup for E-GCLs (wetting from bottom)

The process described above was for "wetting from bottom" tests. For "wetting from top" tests the upper aluminum ring was filled with distilled water using the port located on the ring (Fig. 2b). For the "wetting from top and bottom" tests, both upper and lower aluminum rings were filled with distilled water using the methods described above.

6. DIFFUSION TESTS

a) Test setup

In this part of the study the chloride diffusion coefficients were determined for the E-GCLs and industrial GCLs using the swell-diffusion apparatus. Diffusion tests were performed after the E-GCL sample gained its full swell during the swelling process as described above. The swelled sample remained undisturbed in the apparatus before performing the diffusion test on the sample. After termination of the swelling process, the lower aluminum ring, which will be called the "source reservoir", was full of distilled water. A sodium chloride solution of known chloride concentration was prepared using a pure sodium chloride salt and was replaced with the distilled water by flushing method. A tank containing the NaCl solution was attached to the inlet valve of the source reservoir and the solution level inside the tank was adjusted to about 1 cm above the bottom of E-GCL. The inlet and outlet valves of the source reservoir were opened simultaneously and the NaCl solution was allowed to flow through the reservoir and to flush the distilled water. The out-flowing chloride concentration of the NaCl solution was monitored during the flushing

process until the chloride concentration was the same as the initial chloride concentration in the tank. When the flushing process terminated, the valves were closed and a burette-pipette setup was assembled and attached to the outlet valve as shown in Fig. 6. Some distilled water was placed on top of a GCL sample and left for few days to produce distilled water which is in equilibrium with GCL. The upper aluminum ring was filled with distilled water through the opening of the top Plexiglas plate until the water height on top of the E-GCL was 3 cm. The term "receptor reservoir" will used for the distilled water reservoir. The diffusion test commenced and the time and initial chloride concentration in the source reservoir were recorded. During the test, chloride diffusion occurred upward from the source reservoir, through the E-GCL, and into the receptor reservoir. Solution samples were taken on a regular basis from the source and receptor reservoirs through the septum ports (see Fig. 2b) to observe the chloride concentration with time in the reservoirs during the test. The observed chloride concentrations in the source and receptor reservoirs were plotted against time as will be discussed later.

The burette-pipette assembly in the diffusion test was considered for solution sampling from the receptor reservoir (Fig. 6). During sampling, the horizontal pipette was filled with distilled water through the vertical burette, the T valve was closed, the outlet valve was opened, and the solution was extracted by a syringe already inserted into the source reservoir through the septum port. During the extraction process the extracted solution was automatically and simultaneously replaced by distilled water flowing from the pipette into the source reservoir. After sampling, the outlet valve was closed and the pipette was refilled for a second sampling.

As shown in Fig. 6, the swell-diffusion cell is located on a magnetic stirrer to continuously rotate a magnetic bar inside the source reservoir to keep a uniform concentration of NaCl solution inside the source reservoir during the test. The receptor reservoir solution was stirred manually through the opening in the top of the Plexiglas plate during the test. The tank in the left side of Fig. 6 is used for the flushing process as described earlier and its valve is closed during the diffusion part of the test. The tests were performed at 23±2 °C room temperature. After termination of the test, source and receptor reservoir solutions were evacuated, the test cell was disassembled, and the GCL sample was exhumed. The final values of porosity, water content, and wet density of the GCL were determined. Each diffusion test was duplicated to ensure the reproducibility of the test results and the results of one test on each GCL sample are presented. The conducted tests for E-GCLs type A will be referred to as Tests SDA1 and SDA2, for type B as Tests SDB1 and SDB2, and for the industrial GCLs types Bentofix-NW and Bentofix-NWL as SDNW and SDNWL, respectively.

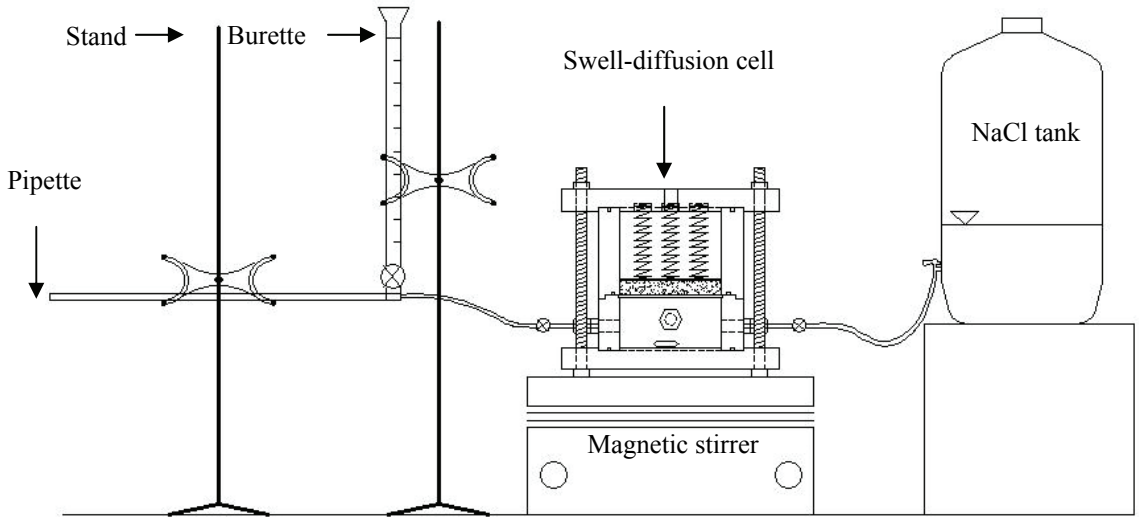

Fig. 6. Schematic of the diffusion test setup for E-GCLs

b) Theoretical model

The chloride ion can migrate through a GCL under a concentration gradient by the process of molecular diffusion. Diffusion through a GCL is essentially the same process as diffusion through a porous medium. The equation describing one dimensional pure diffusive transport (and absorption, where appropriate) can be written as follows:

$$(\theta + \rho K_d)\frac{\partial c}{\partial t} = \theta D\frac{\partial^2 c}{\partial z^2} \tag{1}$$

where c is the contaminant concentration at a depth z at time t; θ is the soil volumetric water content (θ = n, the soil porosity for saturated soil); ρ is the dry bulk density of the soil, K_d is the distribution coefficient (for chloride ion equals to zero), and D is the hydrodynamic dispersion coefficient.

The hydrodynamic dispersion coefficient consists of effective diffusion coefficient, D_e, and mechanical dispersion coefficient, D_{md} , and is given by:

$$D = D_e + D_{md} \tag{2}$$

Diffusion coefficient of a GCL depends predominantly on the bulk void ratio. Lake and Rowe conducted diffusion tests on GCLs with 3-5 g/l solutions of sodium chloride and found a lower diffusion coefficient for lower bulk void ratio [25].

The boundary condition imposed by the source reservoir whose concentration $c_T(t)$ reduces with time due to the movement of chloride into the soil and also sampling, can be modelled by [7]:

$$c_R(t) = c_o - \frac{1}{H_f}\int_0^t f_R d\tau - \frac{q_o}{H_f}\int_0^t c_T(\tau)d_t \tag{3}$$

where c_o is the initial concentration in the reservoir, H_f is the height of fluid in the source reservoir, q_o is the volume of fluid per unit area per unit time removed from the reservoir for chemical analysis during the test and replaced by distilled water, and f_R is the contaminant flux into the soil and is given by:

$$f_R = -\theta D\frac{\partial c}{\partial z} \tag{4}$$

where all the terms are as previously described.

A solution to Eq. (1) which allowed consideration of a finite mass of contaminant in the source, and replacement of sampled reservoir fluid by distilled water (the boundary condition given by Eq. (3), has been given by Rowe and Booker [27], and has been implemented in a computer program POLLUTE [24]. This program, which uses finite layer technique, is used in this study to predict the observed concentration profiles in the tests conducted.

7. RESULTS AND DISCUSSION

a) Swell tests

According to the tree diagram of Fig. 4, the amount of maximum swell for each E-GCL is summarized in Table 3. As described earlier, the industrial GCLs (type Bentofix-NW and Bentofix-NWL) were tested with 12.5 kPa stress and were wetted from top and bottom. The swell data for the industrial GCLs are listed in Table 4. The amount of swell against elapsed time during each swell test was recorded and plotted.

To investigate the effect of stitching on the amount of swell, the results of swell tests A1 and A7 were plotted together as shown in Fig. 7. As can be identified from the figure, the stitching of E-GCL type A caused the maximum swell to be limited to 1.5 mm (Test A7) compared to about 6.0 mm (Test A1) when the E-GCL is not stitched, and shows that stitching minimizes the amount of swell.

To observe the effect of applied stress on the amount of maximum swell, the results of swell tests A7 and A9 were plotted together as shown in Fig. 8. As is observed from the figure, the applied stress of 12.5 kPa caused the maximum swell of E-GCL type A to be limited to 1.2 mm (Test A9) compared to 1.5 mm (Test A7) when there is no stress on the sample. It could be concluded that 12.5 kPa applied stress does not have a significant effect on the E-GCLs swell.

To identify the effect of method of wetting on the amount of swell on the E-GCL samples with no stitch and under the applied stress of 12.5 kPa, the results of swell tests A4 and A6 were plotted together as shown in Fig. 9. As can be observed from the figure, wetting from both sides of the sample (top and bottom) caused the sample to swell slightly more (maximum swell of about 2 mm) compared to one side wetting (maximum swell of about 1.5 when wetted from bottom only). A similar conclusion could be made for Tests A9 and A11 when both samples were stitched and were under stress with differences on the method of wetting (Fig. 10). Two ways of wetting also accelerated the swelling process with respect to time.

To compare the swelling behavior of E-GCLs with industrial GCLs, the results of swell tests NW1, NWL1 (industrial GCLs), and tests A11 and A12 (E-GCLs) are plotted together as shown in Fig. 11. It can be seen from the figure that, on average, the industrial GCLs swelled about 1.5 mm more than the E-GCLs. As described earlier, Bentofix-NW and Bentofix NWL had a 4340 g/m^2 and 3660 g/m^2 high quality granular sodium bentonite layer encapsulated between the geotextile layers compared to a 4440 g/m^2 low quality powdered bentonite layer encapsulated between the geotextile layers. The quality of geotextiles used in these GCLs is not believed to have a critical effect on the amount of swell. The mass per unit area of the sodium bentonite used in E-GCLs was 4440 g/m^2 compared to 4340 g/m^2 and 3660 g/m^2 for Bentofix-NW and Bentofix-NWL, respectively. The difference is not high and is not believed to have a significant effect on the amount of swell, particularly when both industrial GCLs with different amounts of mass per unit area of bentonite showed almost the same amount of swell. The main reason for the lower amount of swell of E-GCLs compared to industrial GCLs could be the quality of bentonite. In E-GCLs the sodium bentonite was powdered with low quality compared to the high quality granular bentonite in industrial GCLs. The method of preparation of the GCLs and other unknown experimental errors could also be attributed to the difference of the maximum swell in E-GCLs and industrial GCLs.

Table 3. Maximum swell for E-GCLs types A and B in swelling tests

Maximum swell for E-GCLs types A & B (mm)											
No stitch						With stitch					
Zero stress		12.5 kPa stress				Zero stress		12.5 kPa stress			
Wetting from top		Wetting from bottom		Wetting from top and bottom		Wetting from top		Wetting from bottom		Wetting from top and bottom	
A1	A2	A3	A4	A5	A6	A7	A8	A9	A10	A11	A12
5.98	4.58	1.50	1.46	1.68	1.98	1.50	1.76	1.22	1.17	1.36	1.42
--	--	--	--	B1	B2	--	--	--	--	B3	B4
--	--	--	--	2.33	2.33	--	--	--	--	1.61	1.65

Table 4. Maximum swell for industrial GCLs (Bentofix-NW and Bentofix-NWL) in swelling tests (numbers are in millimeters)

12.5 kPa stress and wetting from top and bottom			
Bentofix-NW		Bentofix-NWL	
NW1	NW2	NWL1	NWL2
2.90	2.73	2.92	2.85

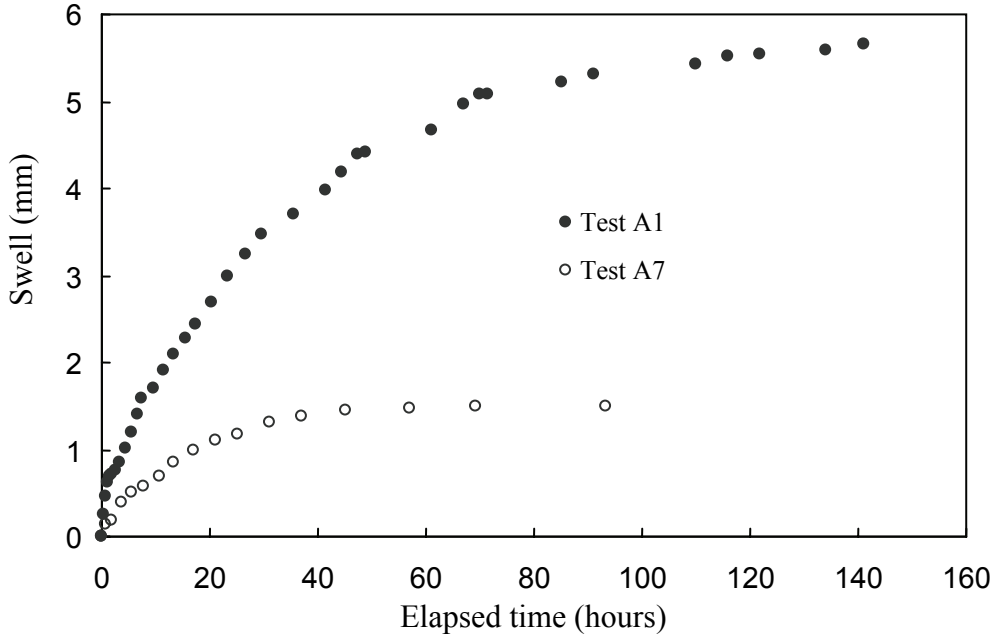

Fig. 7. Results of swell in Tests A1 and A7 (effect of stitching)

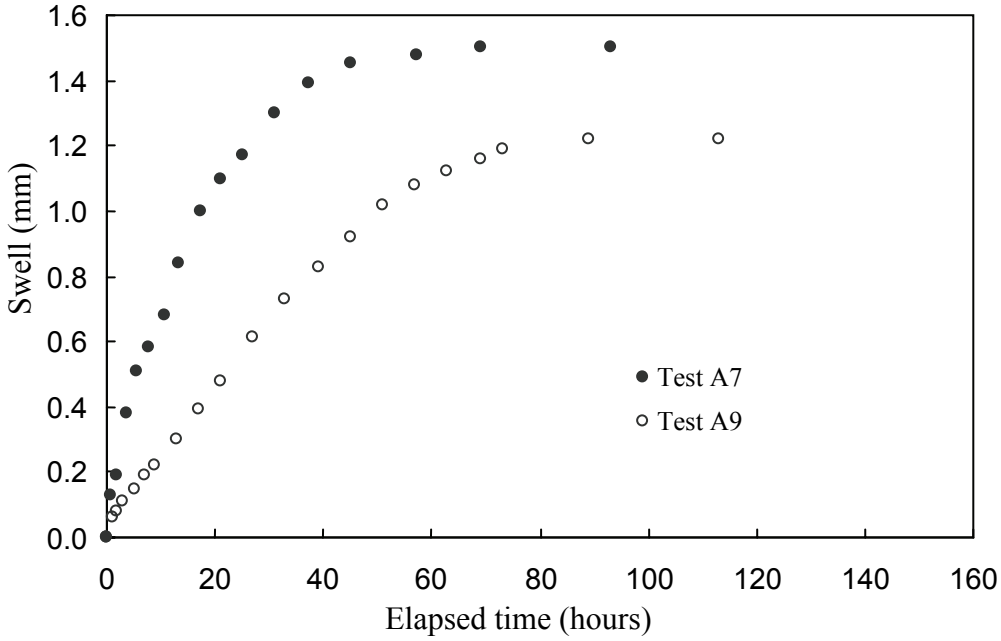

Fig. 8. Results of swell in Tests A7 and A9 (effect of applied stress)

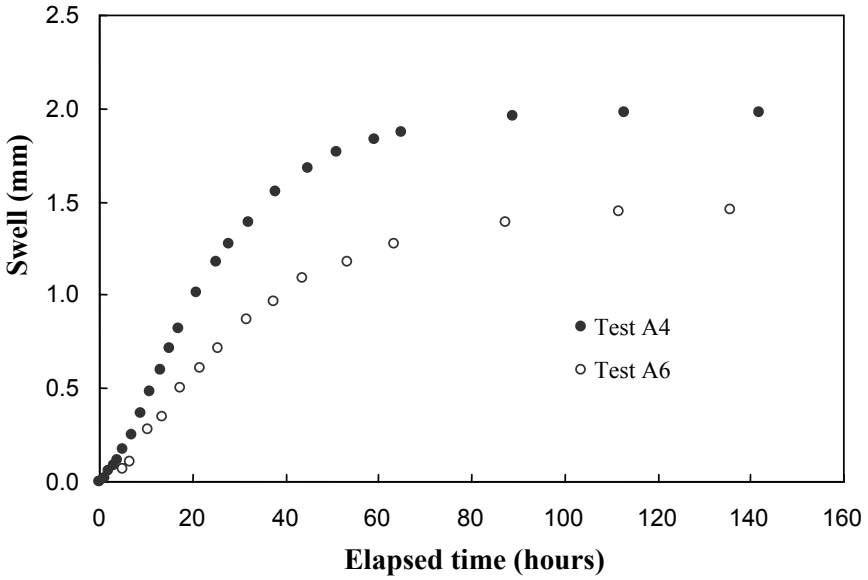

Fig. 9. Results of swell in Tests A4 and A6 (effect of method of wetting – no stitch and 12.5 kPa applied stress)

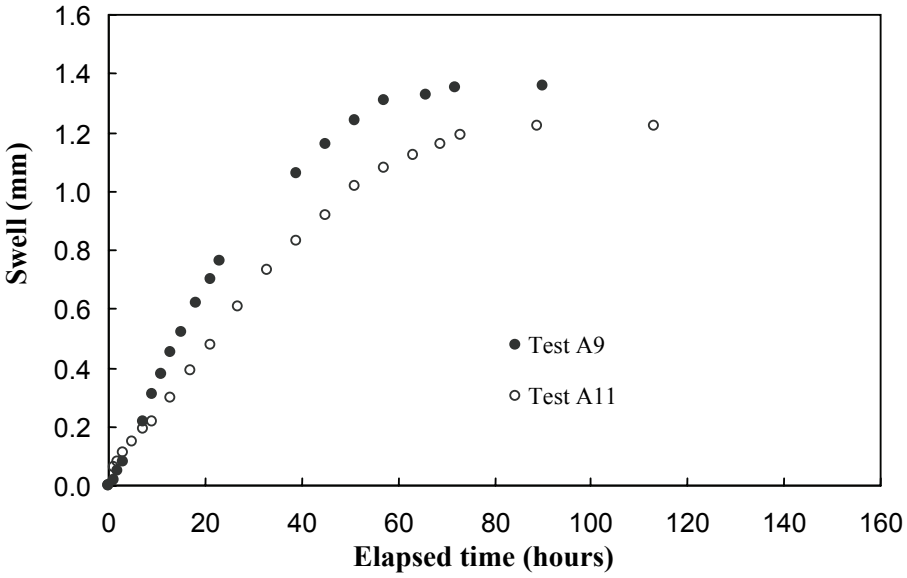

Fig. 10. Results of swell in Tests A9 and A11 (effect of method of wetting – with stitch and 12.5 kPa applied stress)

b) Diffusion tests

The input parameters for theoretical analysis with POLLUTE for diffusion tests SDA1, SDB1, and SDNW are listed in Table 5, as an example. The results of chloride effective diffusion coefficients obtained from all conducted diffusion tests on E-GCLs and industrial GCLs have been summarized in Table 6. The diffusion coefficients were obtained by fitting the theoretical concentration-time data obtained from POLLUTE analysis, and using the geometrical, physical, and chemical tests data (Table 5) into the observed concentration-time data. The effective diffusion coefficient that provided the best fit was selected as the target chloride diffusion coefficient for the tested GCL. As an example, Figs. 12, 13, and 14 show the observed data along with the best fit theoretical concentration-versus time graphs for

diffusion Tests SDA1, SDB1, and SDNW, respectively. As could be verified from these figures, there is good agreement between the observed and theoretical data. The diffusion coefficients obtained for the tested GCLs in this study were in the range of the reported diffusion coefficients by other researchers for comparable products [25].

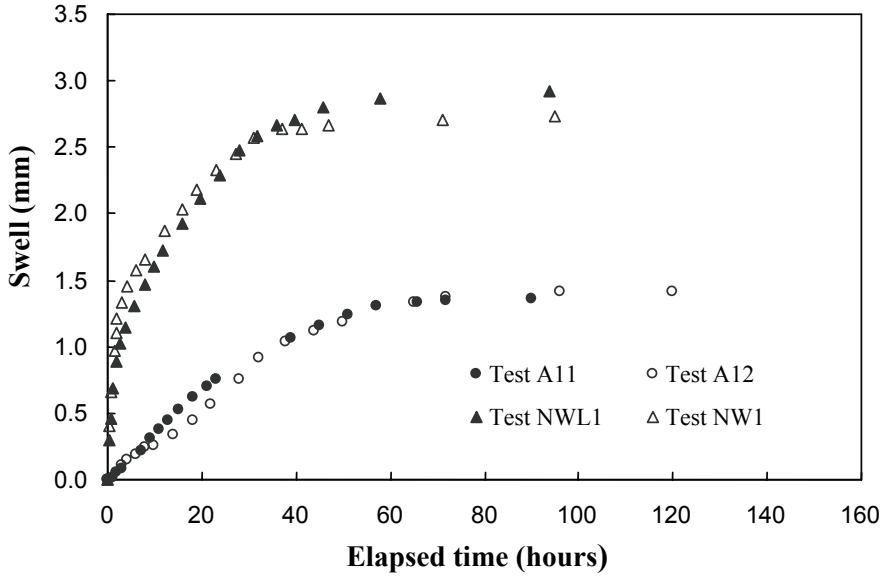

Fig. 11. Comparison of the swelling behavior of E-GCLs with industrial GCLs

Table 5. Input parameters for theoretical analysis with POLLUTE for diffusion tests SDA1, SDB1, and SDNW

Parameter	Test SDA1	Test SDB1	Test SDNW
GCL Thickness (mm)	8.8	9.4	8.7
Height of receptor solution (mm)	30	30	30
[Cl^-] Source solution concentration (mg/L)	1885	1820	1890
[Cl^-] Receptor solution concentration (mg/L)	28	10	9
[Cl^-] Background concentration in GCL (mg/L)	95	95	78
GCL Porosity	0.65	0.73	0.76
GCL dry density (g/cm^3)	0.92	0.69	0.62
Test duration (days)	8.5	14.4	15

Table 6. Chloride diffusion coefficients obtained for E-GCLs and industrial GCLs in diffusion tests (all values in m^2/s)

E-GCLs				Industrial GCLs	
Type A		Type B		Bentofix-NW	Bentofix-NWL
SDA1	SDA2	SDB1	SDB2	SDNW	SDNWL
2.9×10^{-10}	2.7×10^{-10}	2.9×10^{-10}	3.5×10^{-10}	2.9×10^{-10}	3.5×10^{-10}

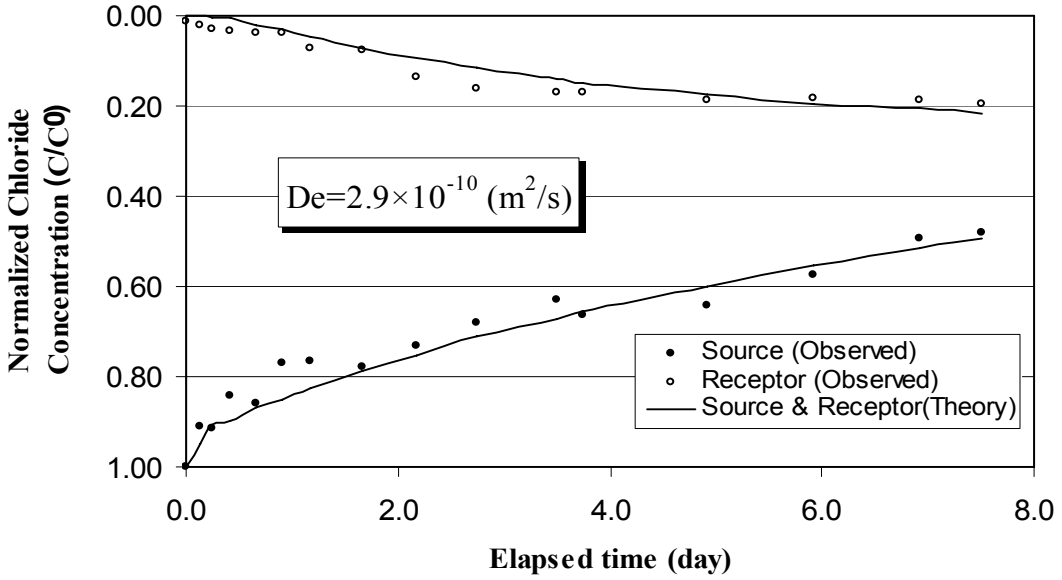

Fig. 12. Observed and predicted normalized chloride concentrations against elapsed time in diffusion test No. SDA1 on E-GCL type A

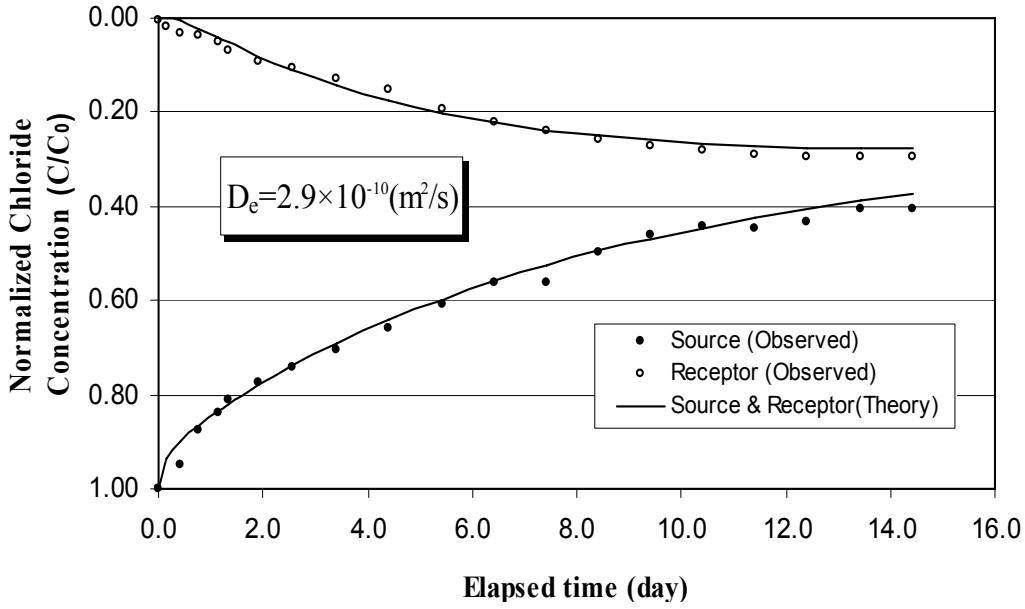

Fig. 13. Observed and predicted normalized chloride concentrations against elapsed time in diffusion test No. SDB1 on E-GCL type B

The chloride diffusion coefficients for E-GCLs types A and B ranged from $2.7\text{x}10^{-10}$ m^2/s to $3.5\text{x}10^{-10}$ m^2/s, and diffusion coefficients of $2.9\text{x}10^{-10}$ m^2/s and $3.5\text{x}10^{-10}$ m^2/s were obtained for the industrial GCLs. These values are in the range of the reported values for comparable GCLs. Two conclusions could be made from these results. First, the difference in the values of diffusion coefficients are small and show that the differences in GCL types, their component types, and their method of production (laboratory or industrial) has no significant effect on diffusion results. Second, the reasonable agreement of diffusion coefficients of E-GCLs and industrial GCLs confirm the quality of the laboratory made GCLs and the methodology used for the diffusion tests.

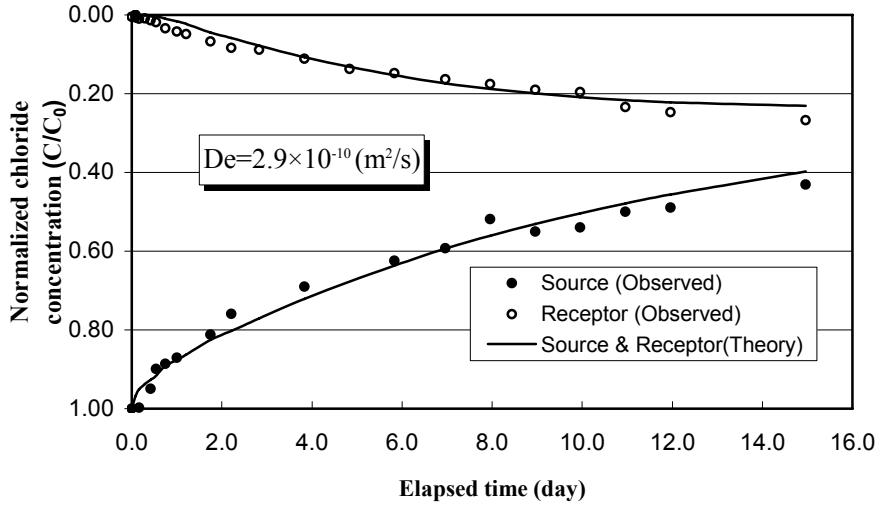

Fig. 14. Observed and predicted normalized chloride concentrations against elapsed time in diffusion test No. SDNW on Bentofix NW

8. SUMMARY AND CONCLUSIONS

Two types of GCLs were fabricated in the laboratory (E-GCLs) to examine the productivity of the GCLs in laboratory scale using local materials. A swell-diffusion apparatus was designed and fabricated to investigate the behavior of the E-GCLs for swelling and diffusion. Two types of industrial GCLs were also tested for comparison purposes. The sodium bentonite used in E-GCLs production was tested for its index parameters and was identified as low quality bentonite. The effect of stitching, applied stress, and method of wetting on the E-GCLs was investigated and the results showed that stitching effectively minimizes the amount of swell, but the applied stress up to 12.5 kPa has no significant effect on the GCLs swell. The wetting from top and bottom caused the E-GCLs to swell slightly more and the swelling process to be accelerated compared to one way swelling. The industrial GCLs swelled more than the E-GCLs which could be due to the high quality granular sodium bentonite used in industrial GCLs compared to the low quality powdered sodium bentonite used in E-GCLs.

The chloride diffusion coefficients obtained for E-GCLs and industrial GCLs ranged from 2.7×10^{-10} m^2/s to 3.5×10^{-10} m^2/s. There was a good agreement between the results obtained for E-GCLs and industrial GCLs in this study with those reported in the literature for similar products and confirm the accuracy of the test apparatus and the adopted test methodologies.

REFERENCES

1. Bouazza, A. (2002). Geosynthetic clay liners. Review article, *Geotextiles and Geomembranes,* Vol. 20, pp. 3-17.
2. U.S. EPA (1997). Geosynthetic clay liners used in municipal solid waste landfills. *United States Environmental Protection Agency*, Report No. EPA 530-F-97-002.
3. Rowe, R. K. & Badv, K. (1996). Use of a geotextile separator to minimize intrusion of clay into a coarse stone layer. *Geotextiles and Geomembranes*, Elsevier Science Limited, Vol. 14, pp. 73-93.
4. Badv, K. & Abdolalizadeh, R. (2004). A laboratory investigation on the hydraulic trap effect in minimizing chloride migration through silt. *Iranian Journal of Science and Technology*, *Transaction B*, Vol. 28, No. B1, pp. 107-118.
5. Badv, K. & Mahooti, A. A. (2004). Advective-diffusive and hydraulic trap modeling in two and three layer soil systems. *Iranian Journal of Science and Technology*, *Transaction B*, Vol. 28, No. B5, pp. 559-572.

6. Rowe, R. K. (2001). *Liner systems, chapter 25 of geotechnical and geoenvironmental engineering handbook*. Kluwer Academic Publishing, Norwell, U.S.A., pp. 739-788.
7. Rowe, R. K., Booker, J. R. & Quigley, R. M. (1995). *Clayey barrier systems for waste disposal facilities*. E & F N Spon (Chapman & Hall), London, p. 390.
8. Badv, K. & Omidi, A. (2007). Effect of synthetic leachate on the hydraulic conductivity of clayey soil in Urmia city landfill site. *Iranian Journal of Science and Technology*, *Transaction B: Engineering*, Vol. 31, No. B5, pp. 535-545.
9. Rowe, R. K., Quigley, R. M., Brachman, R. W. I. & Booker, J. R. (2004). *Barrier systems for waste disposal*, 2nd ed., Spon Press, London, UK.
10. Gassner, F. W. (2006). Base liner equivalency assessment for landfill sites. *8th International Conference on Geosynthetics*, Yokohama, Japan, pp. 193-196.
11. Foose, G. J., Benson, C. H. & Edil, T. B. (1996). Evaluating the effectiveness of landfill liners. *Environmental Geotechnics, Kamon (ed.),* Balkema, Rotterdam, *pp.* 217-221.
12. Bathurst, J. R., Rowe, R. K., Zeeb, B. & Reimer, K. (2006). A geocomposite barrier for hydrocarbons containment in the arctic. *International Journal of Geoengineering Case Histories,* Vol. 1, No. 1, pp. 18-34.
13. Mukonoki, T., Rowe, R. K., Li, H. M., Sangam, H. P., Hurst, P., Bathurst, R. J. & Badv, K. (2003). Hydraulic conductivity and diffusion characterization of GCLs. *Proceedings of the 56th Canadian Geotechnical and 4rd Joint IAH-CNC/CGS and NAGS Conferences,* Manitoba, Canada, pp. 118-125.
14. Bouazza, A., Van Impe, W. F. & Van Den Broeck, M. (1996). Hydraulic conductivity of a geosynthetic clay liner under various conditions. *Environmental Geotechnics, Kamon (ed.)*, Balkema, Rotterdam, pp. 453-457.
15. Kolstad, D. C., Benson, C. H. & Edil, T. B. (2004). Hydraulic conductivity and swell of non-prehydrated geosynthetic clay liners permeated with multispecies inorganic solutions. *ASCE Journal of Geotechnical and Geoenvironmental Engineering*, Vol. 130, No. 12, pp.1236-1249.
16. Takahashi, S. & Kondo, M. (1996). Evaluation of swelling behavior and permeability of geosynthetic clay liner. *Environmental Geotechnics, Kamon (ed.)*, Balkema, Rotterdam, pp. 609-614.
17. Lake, C. B. & Rowe, R. K. (2000). Diffusion of sodium and chloride through geosynthetic clay liners. *Geotextiles and Geomembranes*, Vol. 18, pp. 103-131.
18. Mukonuki, T. & Rowe, R. K. (2006). Effectiveness of a geocomposite liner to diffusion of aromatic hydrocarbons at low temperature. *8th International Conference on Geosynthetics*, Yokohama, Japan, pp. 163-166.
19. Li, H. M., Rowe, R. K., Bathurst, R. J., Sangam, H. P., Mukonoki, T. & Badv, K. (2002). Installation and monitoring of a geocomposite barrier system on Brevoort Island, *Proceedings of the 55th Canadian Geotechnical and 3rd Joint IAH-CNC and CGS Groundwater Specialty Conferences*, Niagara Falls, Canada, pp. 987-992.
20. Hurst, P. & Rowe, R. K. (2004). Effect of jet fuel on the behavior of unsaturated and saturated frozen GCLs. *57th Canadian Geotechnical Conference*, Quebec, Canada, pp. 23-27.
21. American Society for Testing and Materials (1993). Determining the coefficient of soil and geosynthetic or geosynthetic and geosynthetic friction by the direct shear method. ASTM D 5321.
22. American Society for Testing and Materials (1991). Standard practice for quality control of geosynthetic clay liners, ASTM D 5889.
23. Lee, J. M. & Shackelford, C. D. (2005). Impact of bentonite quality on hydraulic conductivity of geosynthetic clay liners. *ASCE-Journal Geotechnical and Geoenvironmental Engineering*, Vol. 131, No. 1, pp. 64-77.
24. Egloffstein, T. (1995). Properties and test methods to assess Bentonite used in geosynthetic clay liners, *Geosynthetic Clay Liners*. Koerner, R. M., Gartung, E. and Zanzinger, H., Editors, Balkema, *Proceedings of an International Symposium*, *held in Zurnberg, Germany*, April 1994, pp. 51-72.

25. Lake, C. B. & Rowe, R. K. (2000). Diffusion of sodium and chloride through geosynthetic clay liners. *Geotextiles and Geomembranes,* Vol. 18, No. 24, pp. 103-131.
26. Rowe, R. K. & Booker, J. R. (1987). *An efficient analysis of pollutant migration through soil', Numerical methods of transient and coupled systems*. R.W. Lewis, E. Hinton, P. Bettess, and B.A. Schrefler, eds., John Wiley and Sons, Ltd., New York, N.Y., Ch. 2, pp.13-42.
27. Rowe, R. K. & Booker, J. R. POLLUTE v.6.: © (1983, 1990, 1994). *1D pollutant migration through a non-homogeneous soil*. Distributed by GAEA Environmental Engineering Ltd., 44 Canadian Oaks Drive, Whitby, Ontario, Canada.